JAERI-M
87-177

LOWER HYBRID CURRENT DRIVE MODELS AND THEIR VERIFICATION WITH ASDEX DATA
—CONCEPTUAL DESIGN STUDY OF FY86 FER—

October 1987

Ken YOSHIOKA*, Hideaki MATSUURA**, Takashi OKAZAKI*
Takumi YAMAMOTO, Masayoshi SUGIHARA and
Noboru FUJISAWA

日本原子力研究所
Japan Atomic Energy Research Institute

JAERI-M レポートは，日本原子力研究所が不定期に公刊している研究報告書です。
入手の問合わせは，日本原子力研究所技術情報部情報資料課（〒319－11 茨城県那珂郡東海村）あて，お申しこしください。なお，このほかに財団法人原子力弘済会資料センター（〒319-11 茨城県那珂郡東海村日本原子力研究所内）で複写による実費頒布をおこなっております。

JAERI-M reports are issued irregularly.
Inquiries about availability of the reports should be addressed to Information Division, Department of Technical Information, Japan Atomic Energy Research Institute, Tokai-mura, Naka-gun, Ibaraki-ken 319-11, Japan.

編集兼発行　日本原子力研究所
印　　刷　山田軽印刷所

JAERI-M 87-177

LOWER HYBRID CURRENT DRIVE MODELS AND THEIR VERIFICATION WITH ASDEX DATA — CONCEPTUAL DESIGN STUDY OF FY86 FER —

Ken YOSHIOKA*, Hideaki MATSUURA**, Takashi OKAZAKI*
Takumi YAMAMOTO+, Masayoshi SUGIHARA and Noboru FUJISAWA

Department of Large Tokamak Research
Naka Fusion Research Establishment
Japan Atomic Energy Research Institute
Naka-machi, Naka-gun, Ibaraki-ken

(Received October 7, 1987)

Two models for evaluating the lower hybrid current drive efficiency in the presence of a DC electric field are developed and their results are compared with experimental data from the ASDEX tokamak. The first model is based on an one-dimensional Fokker-Planck equation combined with a radial wave propagation equation. The second model is an extension of the two-dimensional "adjoint model" which was originally developed by Fisch and Karney.

The calculated steady state (zero DC electric field) current drive efficiency defined by the amount of driven current per unit absorbed of power agrees within 30% error with the experimental data for each of the two models. However, the one-dimensional Fokker-Planck model fails to predict a dependence of current drive efficiency on the DC electric field, whereas the dependence predicted by the adjoint equation model agrees well, being within the experimental error.

Keywords: Lower Hybrid Waves, Current Drive, ASDEX, Transformer Recharge, Current Startup, Fokker-Planck Equation, Adjoint Method

+ Department of Thermonuclear Fusion Research
* Energy Research Laboratory, Hitachi Ltd.
** Faculty of Engineering, Kyushu University

JAERI－M 87－177

低域混成波電流駆動モデルの開発とASDEX実験データによる検証
―次期大型装置設計（FY 86 FER）―

日本原子力研究所那珂研究所臨界プラズマ研究部
吉岡　健[*]・松浦　秀明[**]・岡崎　隆司[*]・山本　巧[+]
杉原　正芳・藤沢　登

（1987年10月7日受理）

低域混成波電流駆動のモデルを開発し，ASDEXの実験データで検証した。開発したモデルは，(1)1次元Fokker－Planck方程式に基づく数値コードと，(2)Fisch－Karney方程式を拡張した解析モデルの2種類である。

トロイダル方向直流電場が零の定常電流駆動効率（高周波電力当りの駆動電流）は，いずれのモデルにても計算値は実験値と30％以内で一致する。トロイダル直流電場が存在するときの駆動効率については，1次元Fokker－Planckコードでは直流電場に対する依存性をうまく捕えられないのに対して，Fisch－Karney方程式を拡張した解析モデルは依存性を良く再現することが分かった。

那珂研究所：〒311－02 茨城県那珂郡那珂町大字向山801－1
＋　核融合研究部
＊　株式会社日立製作所　エネルギー研究所
＊＊ 九州大学工学部

Contents

目　　次

1. Introduction

A "quasi-steady state" operation using rf waves in combination with the transformer has been recently planned for the next generation fusion experimental reactor (FER)[1]. In this mode of operation, lower hybrid waves are used for driving plasma current during the current start-up and transformer recharge phase, whereas the transformer is used mainly during the burn phase. In the former phase, the induced DC toroidal electric field significantly influences the nature of the lower hybrid current drive. A reliable model of rf current drive which takes into account this DC electric field effect is needed for reliable fusion reactor design. Such a model is presented here.

Theories on lower hybrid current drive under the influence of a DC electric field have been proposed by several authors.[2-5] In the first study[2], a fundamental scaling of the current drive efficiency on the DC field was clarified on the basis of an analytical solution to the one-dimensional Fokker-Planck equation. A similar treatment was developed by us[3),4] and is incorporated into a numerical code on radial wave propagation as discussed later.

For a more precise evaluation of current drive with a DC electric field, however, the pitch angle scattering effect of high energy tail electrons becomes essential, and this cannot be treated within the framework of the 1-D Fokker Planck theory. Fisch and Karney[5-7] have included this effect by numerically solving an adjoint equation to the 2-D Fokker-Planck equation, or equivalently solving the Langevin equation[6]. This adjoint theory has been compared with the experimental data from ASDEX[8], PLT[4], and ALCATOR-C[10] and excellent agreement has been confirmed.

However, the above agreement was obtained by adjusting two fitting parameters on the rf wave spectrum of the $n_{/\!/}$ (parallel refractive index) space and rf power absorption. This fitting arises from the fact that the Fisch-Karney adjoint model gives only the current drive efficiency when the rf wave spectrum is localized in the $n_{/\!/}$ space, whereas actual, experimental spectra have a broad profile extending from $n_{/\!/} = 1.2$ to several. (Such broadness arises from the wave guide spectrum itself as well as the unknown spectrum broadening during wave propagation through the plasma.) Instead of introducing

fitting parameters, such uncertainties may be eliminated by averaging the local efficiency over the wave spectrum with a proper weighting function. We take this approach in the present paper to introduce a new analytical expression for current drive efficiency. For this purpose, we seek an analytical solution to the "adjoint equation" for which solutions have only been found numerically up to now.

The purposes of the present paper are the development of two models for lower hybrid current drive and their comparison with experimental data from the ASDEX tokamak. The two models include the above mentioned 1-D Fokker-Planck numerical model and the extended Fisch-Karney's adjoint model. In comparison with experiments, the unknown spectrum broadening effect in the plasma is taken into account by adjusting the wave guide spectrum such that the driven current with zero DC electric field must agree with the experimental value. The comparison results indicate that the proposed extended Fisch-Karney model shows good agreement with experiments without any parameter fitting.

In Section 2, the two models for LH current drive are formulated and comparisons with ASDEX data are presented in section 3.

2. Models

2.1 1-D Fokker-Planck numerical model

In this numerical model, a radial profile of driven current $J_N(r)$ is evaluated by simultaneously solving two equations; the equation for radial wave propagation and the 1-D Fokker-Planck equation which determines the electron velocity distribution at each radial position under the influence of a DC electric field.

The 1-D Fokker-Planck equation for the electron distribution $F(u_{/\!/},r)$ of a given radial position r is given by

$$\frac{d}{du_{/\!/}} D(u_{/\!/}) \frac{dF}{du_{/\!/}} + \frac{Z+2}{2} \frac{d}{du_{/\!/}} \frac{1}{u_{/\!/}^3} \left(\frac{dF}{du_{/\!/}} + u_{/\!/} F \right) - E_N \frac{dF}{du_{/\!/}} = 0, \qquad (1)$$

where $u_{/\!/} = v_{/\!/}/v_{th}$, the toroidal velocity normalized by the electron thermal velocity, v_{th}; $D \equiv D_{QL}/\nu_o v_{th}^2$,[11] the normalized diffusion coefficient proportional to the square of the rf electric field; and $E_N = E_{/\!/}/E_{DR}$, the toroidal DC electric field normalized by the Dreicer field $E_{DR} = m \nu_o v_{th}/e$. Further, $\nu_o = n_e e^4 \ell n\Lambda/2\pi\varepsilon_o^2 m^2 v_{th}^3$, the electron collision frequency; $\ell n\Lambda$ is Coulomb's logalithm; ε_o is the dielectric constant; and e, m, n_e are the electron's charge, mass, and density, respectively.

The absorbed rf power density $P_N(r)$ and its spectrum in the velocity space $P_N(u_{/\!/},r)$ are evaluated from the solution of Eq.(1) as

$$\begin{aligned} P_N(r) &= K \int du_{/\!/} P_N(u_{/\!/},r) \\ P_N(u_{/\!/},r) &= u_{/\!/} D(u_{/\!/}) \frac{dF}{du_{/\!/}} \end{aligned} \qquad (2)$$

where the power density $P_N(r)$ is normalized by $(m n_e v_{th}^2 \nu_o)$ and K=0.392 is the correction factor on the basis of a 2-D Fokker-Planck simulation.[11]

The rf driven current normalized by $(e n_e v_{th})$ is evaluated by

$$J_N(r) = \int du_{/\!/} u_{/\!/} [F(u_{/\!/},r) - F_E(u_{/\!/})] \quad , \qquad (3)$$

where $F_E(u_{/\!/})$ denotes the electron distribution without the rf wave field and is given analytically by $F_E(u_{/\!/}) = \exp(-u_{/\!/}^2/2 + E_N u_{/\!/}^4/4)$.

Using the rf power spectrum $P_N(u_{/\!/},r)$ obtained from Eq.(2) at each radial position r, the radial rf power flux $\Gamma_r(u_{/\!/}, r)$ are calculated through

$$\frac{1}{r}\frac{d}{dr}\Gamma_r = -P_N(u_{/\!/},r)(m\, n_e\, v_{th}^2\, \nu_o) \quad , \tag{4}$$

and the rf diffusion coefficient $D(u_{/\!/})=D_{QL}/\nu_o\, v_{th}^2$, which must be used in Eq.(1), is evaluated through the following expressions:

$$\begin{aligned} D_{QL}(u_{/\!/},r) &= \frac{e^2}{m^2}\,|E|^2\,\frac{\pi}{\omega/u_{/\!/}} \\ \Gamma_r &= v_g\,\omega\,\frac{\partial\varepsilon_r}{\partial\omega}\,\frac{|E|^2}{2} \end{aligned} \tag{5}$$

where E is the rf wave electric field; v_g is the wave group velocity; ω is the wave frequency; and ε_r is the plasma dielectric function.[11]

As a consequence, Eqs.(1) and (4) are dependent on each other through the quantities $P_N(u_{/\!/},r)$ and $D(u_{/\!/},r)$ and are numerically solved simultaneously. In the limit of uniform plasma with large enough rf power, Eqs.(1) and (4) can be solved analytically and the resulting current drive efficiency J_N/P_N coincides with the formula given by Borrass[2] as

$$\frac{J_N}{P_N} = \frac{(J_N/P_N)_o}{1 - K(J_N/P_N)_o \cdot E_N} \quad , \tag{6}$$

where

$$\left(\frac{J_N}{P_N}\right)_o = \frac{4}{Z+5}\,\frac{u_2^2 - u_1^2}{\ell n(u_2/u_1)} \tag{7}$$

is the current drive efficiency without DC electric field E_N, and u_1 and u_2 are the lower and upper limits of the wave phase velocity between which the rf wave spectrum exists.

2.2 Extended Fisch-Karney model

The equation adjoint to the 2-D Fokker-Planck equation under the presence of a DC as well as rf electric field is given by Karney and

Fisch[7] as

$$-\frac{1}{u_R^2}\frac{dw_s}{du_R}+\frac{1+Z}{2u_R^2}\frac{\partial}{\partial\mu}(1-\mu^2)\frac{\partial w_s}{\partial\mu}+\frac{\partial w_s}{\partial u_{R/\!/}}=-u_{R/\!/} \quad , \tag{8}$$

where $u_R = v/v_R$ is the velocity normalized by the Dreicer velocity $v_R = v_{th}/\sqrt{2E_N}$; $u_{R/\!/}$ is its toroidal component, and $\mu \equiv u_{R/\!/}/u_R$. In the case lower hybrid current drive, only the electrons with $|\mu| \simeq 1$ are pushed by rf waves. In this case, Eq.(8) can be approximated with $|\mu| \simeq 1$:

$$\left(1-\frac{1}{u_R^2}\right)\frac{\partial w_s}{\partial u_R}+\frac{Z+1}{2u_R^2}\frac{\partial}{\partial\mu}(1-\mu^2)\frac{\partial w_s}{\partial\mu}=-u_R\mu \quad . \tag{9}$$

The solution of Eq.(9) to the first order of μ can be found analytically as

$$w_s(u_R,\mu) = -\frac{8}{Z+5}\frac{\mu}{\alpha^2}\left[\frac{\alpha}{2}u_R^2+\ell n\left|1-\frac{\alpha}{2}u_R^2\right|\right] \tag{10}$$

with $\alpha = 12/(Z+7)$.

From the adjoint theory[7], the current drive efficiency J_N/P_N is evaluated using the adjoint solution w_s as

$$\frac{J_N}{P_N}=\frac{1}{E_N}\frac{\int du_R^3\,\Gamma\cdot\nabla w_s}{\int du_R^3\,\Gamma\cdot\nabla\frac{u_R^3}{2}} \quad , \tag{11}$$

where $\Gamma \equiv -D\nabla f(u)$ is the particle flux in the velocity space induced by rf waves, and $f(u)$ is the electron distribution i.e. the solution of the 2-D Fokker-Planck equation. The gradient operator ∇ should be taken with respect to the velocity space. Generally, the solution f can only be obtained numerically. But if we use the analytical solution of the 1-D Fokker-Planck equation (F in Eq.(1)) instead of f, then the flux can be approximated as $\Gamma \sim 1/u_R^2$. Using the flux, Eq.(11) becomes

$$\frac{J_N}{P_N}=\left(\frac{J_N}{P_N}\right)_o\frac{\ell n\left|(1-\alpha E_N u_2^2)/(1-\alpha E_N u_1^2)\right|}{\alpha E_N(u_1^2-u_2^2)} \quad , \tag{12}$$

where u_1 and u_2 are again the lower and upper limits of velocity for the wave spectrum. Confirmation of the validity of using the 1-D solution for the evaluation of flux Γ is needed through a full numerical 2-D Fokker-Planck calculation, which will be reported elsewhere.

In the limit of the weak electric field $|E_N| \ll 1$, Eq.(12) approaches

$$\frac{J_N}{P_N} = \left(\frac{J_N}{P_N} \right)_o \left[1 + \alpha E_N \frac{u_2^2 + u_1^2}{2} \right] \tag{13}$$

and coincides with the "hot conductivity model" of Fisch, i.e. a linearized version of the Fisch-Karney model.[5)]

3. Comparison with experimental data

3.1 Procedure for data evaluation

Experimental data on the lower hybrid current drive of ASDEX were supplied to us for use at the IAEA/INTOR Specialist Meeting on Non-inductive Current Drive held at Garching/West Germany (Sept. 1986). The data are divided into two parts : dataset A shown in Table 1 and dataset B shown in Fig. 1. Dataset B consists of the data on the time derivative of the transformer current $\dot{I}_{OH}$ under constant operation of plasma current I_p as a function of injected rf power P^{RF} and average electron density $\bar{n}_e$. Dataset A consists of the data on ohmic heating power defined by $P_{OH} \equiv I_p V_\ell$ instead of $\dot{I}_{OH}$ as in dataset B, where V_ℓ denotes the one turn voltage.

Relationships between the parameters $\dot{I}_{OH}$, P_{LH}, V_ℓ and $\bar{n}_e$ can be understood by seeing the following circuit equation on a plasma ring:

$$L_p \dot{I}_p + V_\ell = -M \dot{I}_{OH}$$
$$V_\ell = R_p [I_p - I_{rf}(\bar{n}_e, P_{LH})] \quad , \tag{14}$$

where L_p and R_p are the inductance and resistivity of plasma; M is the plasma-transformer mutual inductance; and $I_{rf}(\bar{n}_e, P_{LH})$ is the rf driven current as a function of density $\bar{n}_e$ and injected power P_{LH}.

In Eq.(14), we have neglected the contribution from $\dot{L}_p I_p$, i.e. the term for inductance variation due to the current profile variation within the plasma. However, several shots, in which $\dot{L}_p$ has been measured, indicate that the term $\dot{L}_p I_p$, can introduce an error of about 20% in the value of V_ℓ. Since the $\dot{L}_p$ measurement is not available for all the data at this point, this term has been omitted.

We transform the raw experimental data into the normalized current drive efficiency (J_N/P_N) as a function of E_N. By doing this, we can plot the various data with different electron densities in a single graph and compare them with theoretical curves. In the following, the procedures for this transformation are described.

The normalized efficiency (J_N/P_N) can be evaluated with the driven current I_{rf} and injected power P_{LH} as;

$$\frac{J_N}{P_N} = \frac{I_{rf}}{P_{LH}} \, 2\pi R \, E_{DR} \tag{15}$$

where R is the major radius and we assume that all the injected power is absorbed by the plasma. The driven current I_{rf} is evaluated with the experimental data of $\dot{I}_{OH}$ or P_{OH} as

$$I_{rf} = \begin{cases} I_p \left[1 - \dfrac{P_{OH}^{RF}}{P_{OH}^{OH}}\right] \text{------ dataset A} \\ I_p \left[1 - \dfrac{\dot{I}_{OH}^{RF}}{\dot{I}_{OH}^{OH}}\right] \text{------ dataset B} \end{cases} \tag{16}$$

where the superscrips, RF and OH on the rigit of P_{OH} and $\dot{I}_{OH}$ denote "during RF" and "during OH" (without RF).

The normalized field E_N can be evaluated by

$$E_N = \begin{cases} \dfrac{1}{2\pi R \, E_{DR}} \dfrac{P_{OH}^{RF}}{I_p} \text{----- dataset A} \\ \dfrac{1}{2\pi R \, E_{DR}} M \, \dot{I}_{OH}^{RF} \text{----- dataset B} \end{cases} . \tag{17}$$

3.2 Spectrum adjustment

As mentioned in section 1, we adjust the waveguide spectrum such that the driven current I_{rf} must conincide the experimental value of 300 kA. We do this on the steady state current drive shot with $V_\ell = 0$ (No.18468 in Table 1) and then compare all the experimental data with theory using this adjusted spectrum.

The spectrum is adjusted in the same manner as Succi[12] et al. did. Namely, as shown in Fig. 2, we add a triangular "wing" spectrum with width W to the main "wave guide" spectrum and adjust the size of the triangular wing i.e. W and n_{max} such that I_{rf} becomes 300 kA. The results of adjustment calculated using the 1-D Fokker-Planck numerical model are shown in Fig. 3. The driven current I_{rf} is calculated with various n_{max} as a function of W. From the figure, we see that $W \simeq 3.5$ and $n_{max} = 2.6$ are needed for agreement of both experimental and

calculated values.

The resulting rf wave power spectrum is shown in Fig. 4. Curves (a) and (b) correspond to the spectra at the waveguide front and the plasma center, respectively. The triangular wing of our case is somewhat larger than that calculated by Succi et al. for the PETULA-B experiment[12]. The spectrum extends from $n_{/\!/} = 1.5$ to 6.0, and this corresponds to $u_{/\!/} = 4$ to 14 in the velocity space. The calculated radial distribution of driven current is shown in Fig. 5. The current peak is located off-center and this factor qualitatively explains the experimental observation that the current profile generally flattens during rf pulse[8]. However, no further discussions of the current profile is made here, since this requires further consideration of phenomena such as ray propagation to the poloidal direction, ray reflection at the plasma surface and spatial diffusion of high energy tail electrons[13].

3.3 Comparison with data

In Table 2, the steady state (E_N=0) current drive efficiencies $\bar{n}_e I_{rf}/P_{LH}$ (proportional to $(J_N/P_N)_o$) are compared. The theoretical estimations by 1-D Fokker-Planck and extended Fisch-Karney models agree with the experimental value within 30%. These results should be compared with the same analysis on the ASDEX data by Leuterer et al.[8], in which spectrum broadening i.e. the triangular wing in Fig. 4 is not considered and the theoretical estimation is 2.5 times larger than the experimental value.

We proceed now to the more intrinsic part of this analysis, i.e. the dependency of efficiency (J_N/P_N) normalized by the steady state efficiency $(J_N/P_N)_o$ is plotted as a function of toroidal DC field E_N. The plus direction in E_N implies the co-direction, in which the direction of rf acceleration coincides with that of DC field acceleration.

In the figure, the high density data (six shots with $\bar{n}_e \geq 1.6\times10^{13}$ cm^{-3}) are not listed because these data belong to the density regime near the "density cut-off" and their efficiency degrades non-linearly. In fact, as shown in Fig. 7, the sideband signal (PDI) is indicating parametric instability, increasing beyond $\bar{n}_e = 1\times10^{13}$ cm^{-3}.

Returning back to Fig. 6, generally, the 1-D Fokker-Planck model fails to predict the experimental dependency of the current drive efficiency on DC electric field E_N whereas it is predicted by the extended Fisch-Karney model, with agreement being within the experimental scattering. This agreement arises from the consideration of the electron's pitch angle scattering effect which cannot be treated in the 1-D Fokker-Planck model. The high-energy tail electrons generated by the rf can easily change their pitch angles towards the direction of the DC electric field without changing their energies. Then, when the DC electric field is co-directional with the rf field, the current drive efficiency is enhanced more, and when the DC field is counter-directional, the efficiency is degraded more than those estimated by the 1-D model.

In the region near E_N=-0.01, there appears to be a systematic error between experiments and the extended Fisch-Karney model. We consider this as due to the use of the approximate flux Γ as in Eq.(11). For a more precise flux, we need a full numerical Fokker-Planck simulation which is beyond the scope of the present paper.

In Fig. 8, the estimations by the original Fisch-Karney model and our extended Fisch-Karney model are compared. Since the current drive efficiency in the original model is obtained for a localized rf wave spectrum we get different curves for different wave localizations with respect to the wave phase velocity $u_{/\!/} = c/n_{/\!/}v_{th}$. We plot the curves by dashed lines in Fig. 8 for two extreme cases $u_{/\!/} = 4$ and $u_{/\!/} = 14$ (i.e. $n_{/\!/} = 1.5$ to 6) between which the real wave spectrum exists. We also plot the case $u_{/\!/} = 10$ which is the best fit to the extended Fisch-Karney model (solid line). Comparing both curves, the curvature of the extended Fisch-Karney model appears to be larger than that of the original, indicating the larger sensitivity dependence on the DC electric field in the extended model.

4. Conclusion

Two models for the evaluation of lower hybrid current drive efficiency were developed; the 1-D Fokker-Planck numerical model and the extended Fisch-Karney model. These models were compared with experiments on the ASDEX tokamak. Results are summarized as follows:

(1) The steady state (with zero toroidal DC electric field) current drive efficiencies estimated by both models agreed with the experimental data within a 30% error.

(2) As for the dependency of efficiency on the DC electric field, the 1-D Fokker-Planck model failed to predict the correct dependency, whereas the dependency predicted by the extended Fisch-Karney model agreed well with the experimental values, and was within the scattering of data.

Acknowlegement

We would like to thank Drs. F. Leuterer, F. Engelmann and J. G. Wégrowe of the NET Team, Garching, West Germany, for preparing the datasets on ASDEX lower hybrid experiments. We also thank Drs. M. Brambilla and F. X. Söldner for fruitful discussions.

4. Conclusion

Two models for the evaluation of lower hybrid current drive efficiency were developed; the 1-D Fokker-Planck numerical model and the extended Fisch-Karney model. These models were compared with experiments on the ASDEX tokamak. Results are summarized as follows:

(1) The steady state (with zero toroidal DC electric field) current drive efficiencies estimated by both models agreed with the experimental data within a 30% error.

(2) As for the dependency of efficiency on the DC electric field, the 1-D Fokker-Planck model failed to predict the correct dependency, whereas the dependency predicted by the extended Fisch-Karney model agreed well with the experimental values, and was within the scattering of data.

Acknowlegement

We would like to thank Drs. F. Leuterer, F. Engelmann and J. G. Wégrowe of the NET Team, Garching, West Germany, for preparing the datasets on ASDEX lower hybrid experiments. We also thank Drs. M. Brambilla and F. X. Söldner for fruitful discussions.

References

1) Department of Large Tokamak Research, "Conceptual Design Study of Quasi-Steady State Fusion Experiment Reactor (FER-Q) Part 1", JAERI-M 85-178 (1985).

2) K. Borrass and A. Nocentini, Plasma Physics and Controlled Fusion 26, 1299 (1984).

3) T. Okazaki, M. Sugihara, and N. Fujisawa, Nucl. Fusion 28 (1986) 1029.

4) T. Okazaki, M. Sugihara, and N. Fujisawa, Compter Physics Communication 40, 131 (1986).

5) N. J. Fisch, Phys. Fluids 29, 245 (1985).

6) N. J. Fisch, Phys. Rev. Lett. 54, 897 (1985).

7) C. F. F. Karney and N. J. Fisch, Phys. Fluids 29, 180 (1986).

8) F. Leuterer et al., Plasma Physics and Controlled Fusion 27, 1399 (1985).

9) C. F. F. Karney, N. J. Fisch, and F. C. Jobes, Physical Review A 32, 2554 (1985).

10) Y. Takase, "Plasma Current Ramp-Up and OH Recharging Experiments at High Densities on Alcator-C", IAEA/INTOR Specialist Meeting on Non-inductive Current Drive. Garching, Sept. 1986.

11) D. A. Ehst, Nucl. Fusion 19, 1369 (1979); C. F. F. Karney and N. J. Fisch, Phys. Fluids 22, 1817 (1979).

12) S. Succi, et al., in Plasma Physics and Controlled Nuclear Fusion Research, Vol. I, p549 (1984) IAEA Viena.

13) P. Bonoli and R. C. Englade, Phys. Fluids 29, 2937 (1986).

Table 1 ASDEX lower hybrid current drive experiment dataset A

Shot number	$\bar{n}_e$ $10^{13}cm^{-3}$	P_{LH} kW	P_{OH} kW	T_{e0} eV	T_{i0} eV	n_{e0} $10^{13}cm^{-3}$
18470	0.6	90	OH: 260	1820	395	0.74
			LH: 100	1640	480	0.82
18468	0.55	375	OH: 260	1715	425	0.67
			LH: 0	27200	370	0.69
18466	0.5	920	OH: 260	1715	475	0.73
			LH: -45	2620	475	0.61
19612	1.0	90	OH: 230	1540		1.2
			LH: 120	1540		1.32
19617	0.9	815	OH: 238		500	
			LH: 40		550	
18177	1.6	90	OH: 260	1290	685	2.2
			LH: 230	1490	685	2.38
18183	1.6	920	OH: 265	1465	685	2.16
			LH: 140	1780	700	2.35

where I_P=300 kA, B_t=2.2 T, $\bar{n}_l$=2, and D_2 gas were used.

Table 2 Comparison of steady state (E_N=0) current drive efficiencies

	Current drive efficiency $I_P\bar{n}_e/P_{LH}$	
ASDEX experimental data	0.45×10^{13}	[A/Wcm^3]
1-D Fokker Planck model	0.62×10^{13}	
Extended Fisch-Karney model	0.55×10^{13}	

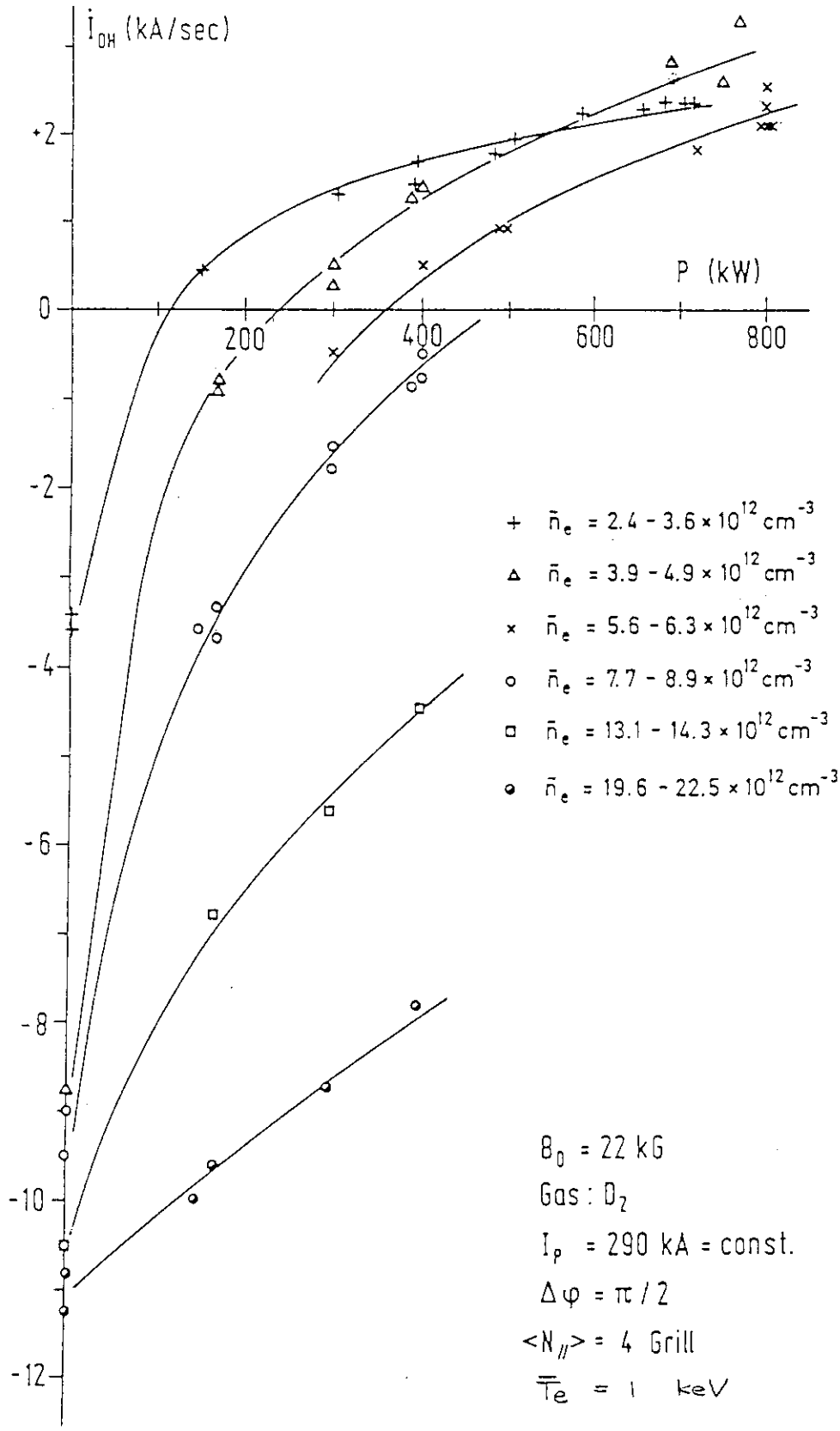

Fig. 1 ASDEX lower hybrid current drive experiment dataset B. The transformer recharge-rates $\dot{I}_{OH}$ are measured as a function of injected rf power P_{LH} for various average densities $\bar{n}_e$.

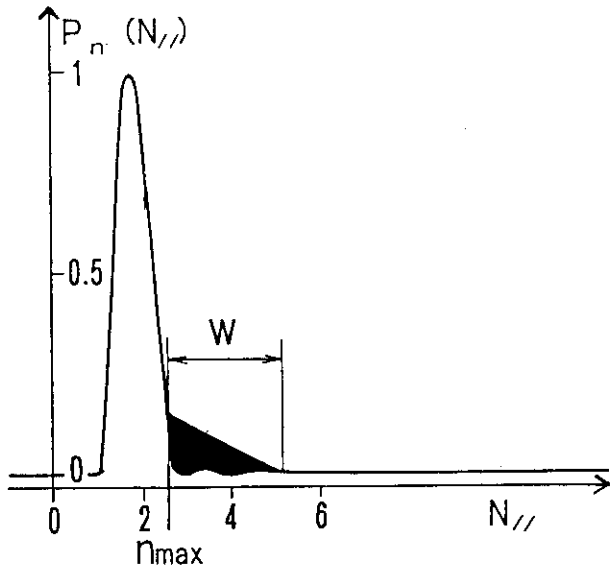

Fig. 2 RF wave power spectrum P_N as a function of parallel refractive index $n_{//}$.

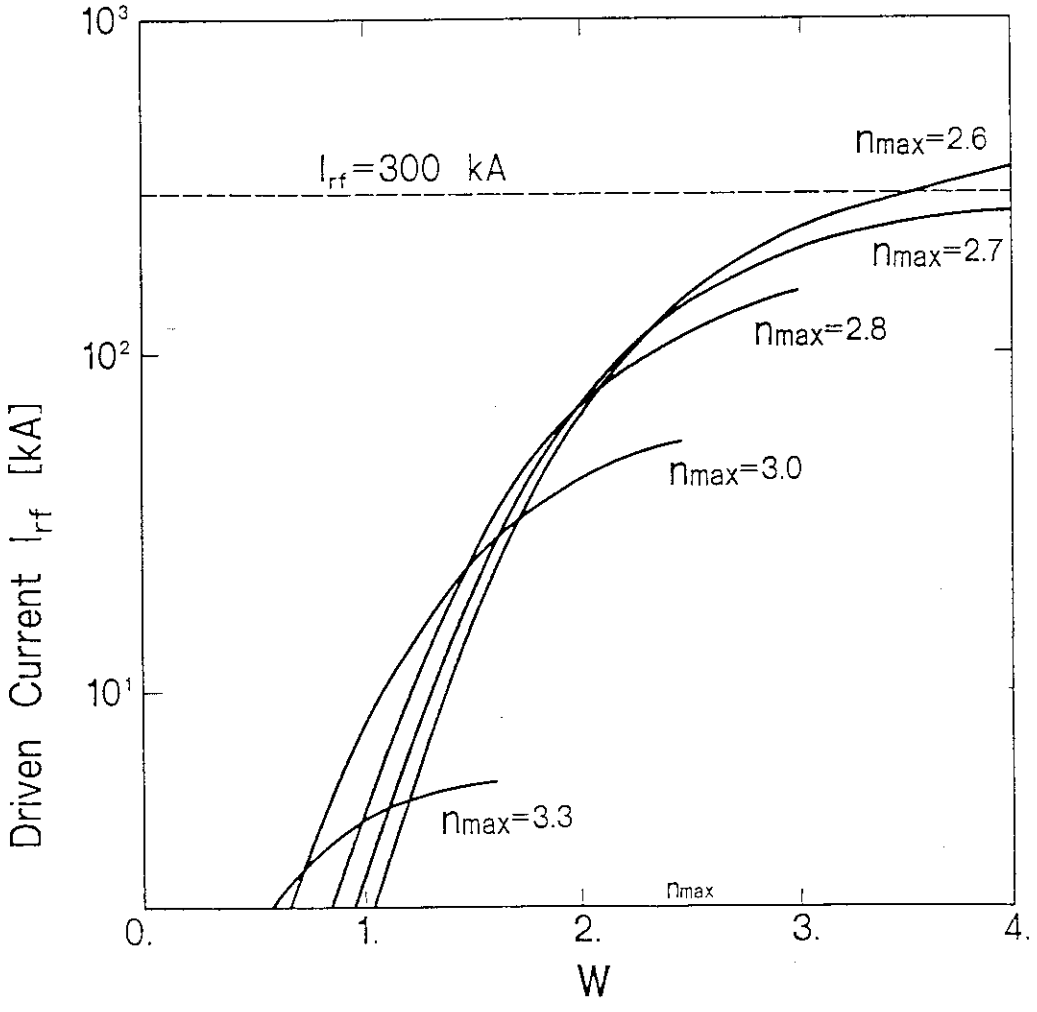

Fig. 3 RF generated current as a function of the width of the triangular wing W.

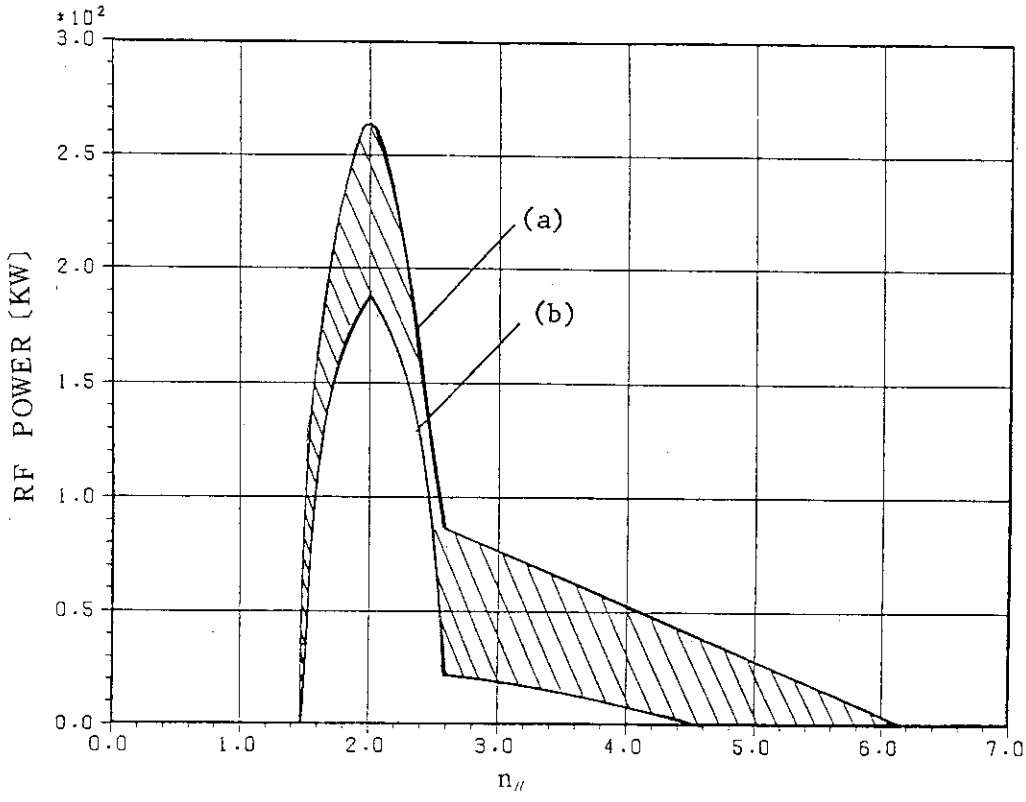

Fig. 4 Resultant rf wave power spectrum after wing adjustment as a function of parallel refractive index $n_{//}$.

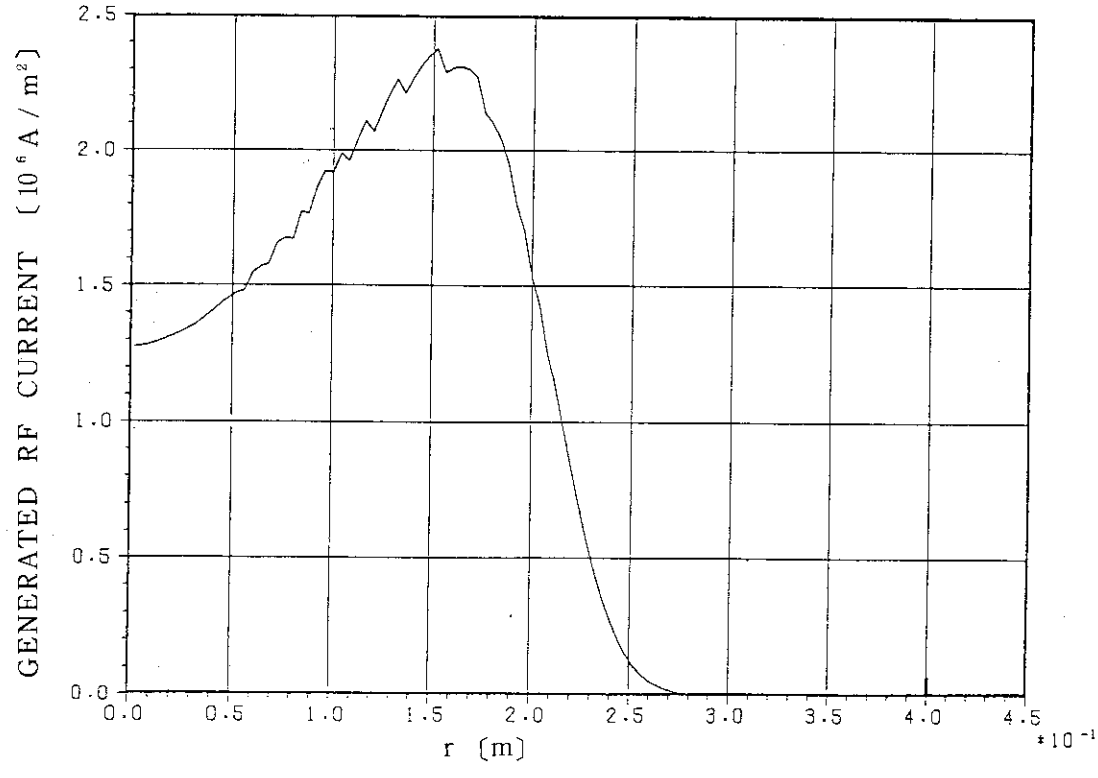

Fig. 5 Radial distribution of rf generated current.

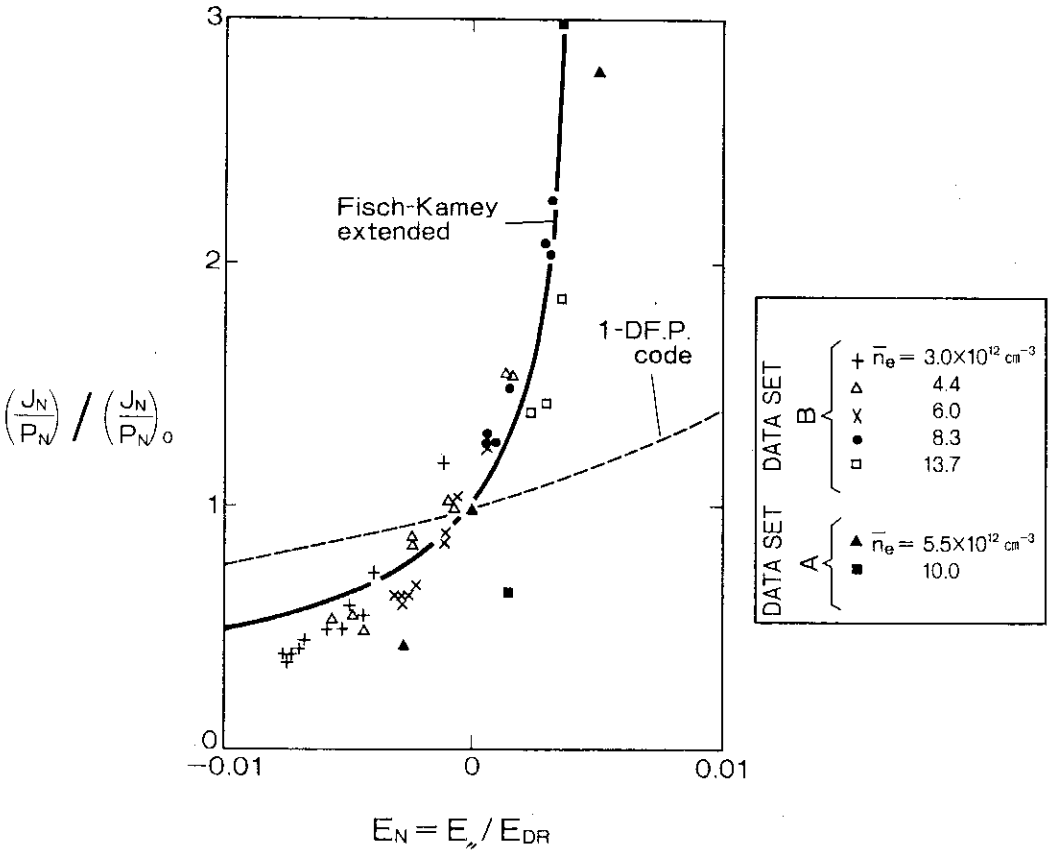

Fig. 6 Comparison of the experimental and theoretical current drive efficiencies. The normalized efficiencies (J_N/P_N) are plotted as a function of DC electric field E_N.

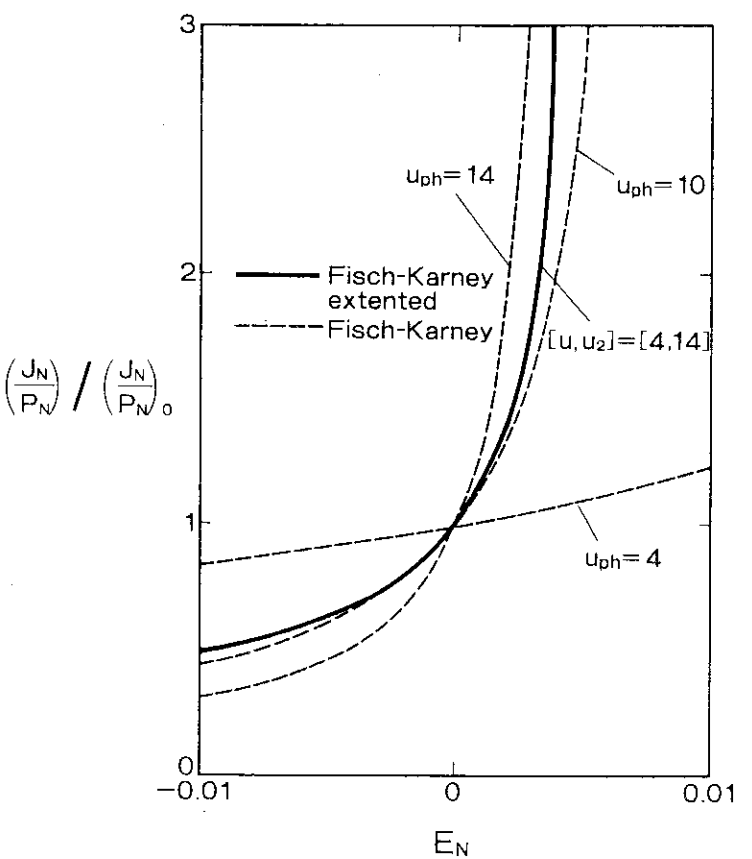

Fig. 8 Comparison of the original Fisch-Karney model and the extended Fisch-Karney model.

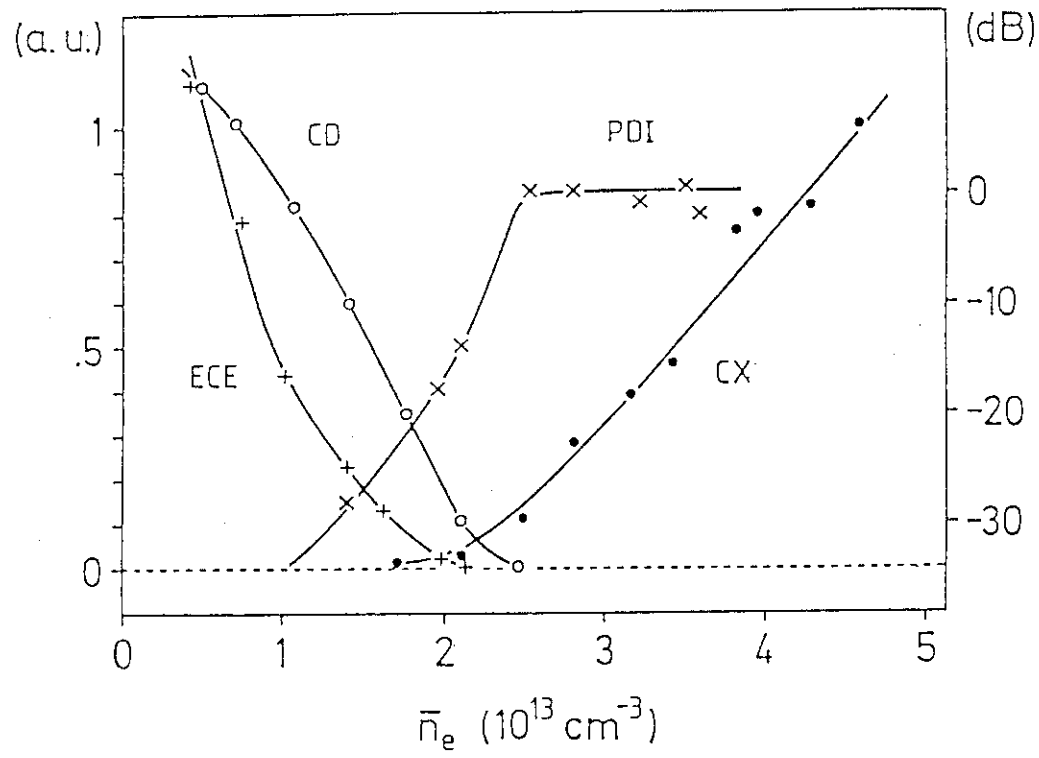

ECE: Amplitude of suprathermal electron cyclotron emission at $2.5\omega_{ce}$

CD: Current drive rate $i_p^{RF} - i_p^{OH}$

PDI: Amplitude of 2nd sideband in the parametric decay spectrum

CX: Flux of $\perp$-ions at E = 8.65 keV.

Fig. 7 Several parameters (ECE, CD, PDI, CX) as a function of electron density $\bar{n}_e$ during rf.